DESIGN AND EXPERIMENTAL OPTIMIZATION OF ROTARY CUTTING SAFFLOWER HARVESTING END EFFECTOR
/
回转切割式红花采收末端执行器设计与试验优化

Puhang LI, Xinyue ZHANG, Hao ZHANG, Zeyu WANG, Shiwei WEN, Jun CHEN*
College of Mechanical and Electronic Engineering, Northwest A&F University, Yangling 712100/China
Tel: +86-13572191773; E-mail: chenjun_jdxy@nwsuaf.edu.cn
DOI: https://doi.org/10.35633/inmateh-71-60

Keywords: *safflower harvesting; rotary cutting tool; end effector; gear transmission; Fluent simulation*

ABSTRACT
Aiming at the problems of high damage rate and loss rate of the existing safflower harvesting equipment, this study designed a rotary cutting safflower harvesting end effector by combining the growth characteristics and mechanical properties. Through force analysis of the cutting tool, the key factors, which affects the harvesting performance, were clarified to be the blade inclination and the knife shaft speed. The Fluent software was used to analyze the flow field of the harvesting chamber, which aims to determine the appropriate wind speed. To improve the working performance of the rotary cutting safflower harvesting end effector, a three-factor, three-level orthogonal test was carried out with the blade inclination, knife shaft speed and wind speed as the influencing factors, and with the recovery rate, damage rate and loss rate as the response indexes. A regression model for the three-factor interaction was developed and optimized based on the results of the Box-Behnken test. The optimal parameter combination is: the blade inclination is 15°, the knife shaft speed is 1570, and the wind speed is 6 m/s. A test of the optimization results showed that the recovery rate was 91.47%, the damage rate was 7.51%, and the loss rate was 4.67%. This study can provide theoretical basis and technical reference for the mechanized harvesting of safflower.

摘要
针对现有红花采收装备存在损伤率高、采净率低等问题，该研究结合红花植株生长特点及力学特性，设计了一种回转切割式红花采收末端执行器。通过对刀具进行受力分析，明确了影响采收性能的关键因素为刀刃倾角和刀轴转速；利用 Fluent 软件对采收腔室流场进行分析，确定适宜的入口风速。为提升回转切割式红花采收末端执行器的工作性能，以刀刃倾角、刀轴转速和入口风速为影响因素，以花丝采净率、损伤率、掉落率为响应指标，进行三因素三水平正交试验。根据 Box-Behnken 试验结果建立了三因素交互作用的回归模型并对其进行优化，获得最优参数组合为：刀刃倾角 15°，刀轴转速 1570rpm，入口风速 6m s^{-1}。对优化结果进行试验验证，结果表明，采净率为 91.47%，损伤率为 7.51%，掉落率为 4.67%。该研究可为红花机械化采收提供理论依据和技术参考。

INTRODUCTION
Safflower is an important cash crop in China, with extremely high value in medical, food and economy (*Ren et al., 2017; Wang et al., 2006; Xue et al. and Li, 2005*). A survey shows that China's safflower planting area has reached 33,300 hectares, and its origin is mainly concentrated in Xinjiang, Yunnan, Gansu, Ningxia, Henan and other regions (*Zhou et al., 2021*).

Recently, the mechanized harvesting of crops has become a hot topic (*Hu et al., 2020, 2021, 2022; Joao et al., 2011; Jobbagy et al., 2021; Pu et al., 2023; Zhang et al., 2021*). In terms of safflower harvesting, scholars have carried out relevant research, and it mainly focus on the methods of pneumatic, pulling, combing, cutting and so on (*Zhang et al., 2019*). *Cao et al.* (*2019*) developed a comb-type safflower harvesting machine, which realized the plucked picking of filaments through the rotating action of the harvesting shaft. This way the mechanized blind harvesting was realized and the efficiency of safflower harvesting was improved, but it had a high rate of missed harvesting. *Zhang et al.* (*2020*) developed a portable roller-type safflower harvester, where the manual hand-held picking head was aligned with the filaments so as to feed the filaments into the rollers, and the pulling force generated by the high-speed rotation of the rollers picked the filaments, which was able to reduce labor intensity and improve the harvesting efficiency. *Zhang et al.* (*2022*) designed a three-finger pull-out safflower picking end effector, where the filaments were harvested by three harvesting fingers using pulling. *Zhang et al.* (*2022*) designed a double-acting opposite direction cutting end effector for safflower harvester, which was driven by a cam to realize the low-speed clamping and cutting of filaments. It effectively reduced the damage rate in harvesting, and realized the low-damage rate of the filaments harvesting.

Above all studies, the damage to the structure of the filaments is the greatest weakness of the existing safflower harvesting devices. In this study, high recovery rate, low damage rate and low loss rate are the design objectives to improve the quality of mechanized safflower harvesting. This study combined the growth characteristics and mechanical properties of safflower to design a rotary cutting safflower harvesting end effector. The structural and motion parameters of the key components were theoretically analyzed. The factors of the performance indexes were determined and the prototype and the field test were carried out, which was intended to provide reference for the design and optimization of safflower harvester.

MATERIALS AND METHODS

Safflower characteristics

Physical properties of safflower are the basis for the design of safflower harvesting end effector. The measurement was carried out at Gongchuang Planting Specialized Cooperative, Yuanzhou District, Guyuan City, Ningxia Hui Autonomous Region, from July 20 to 30, 2023. The main varieties are Yu Hong No. 3, as shown in Figure 1. The five-point method was used for field sampling, and 20 safflower plants in full bloom were selected from each sampling point to obtain the main characteristics of safflower, as is shown in Table 1.

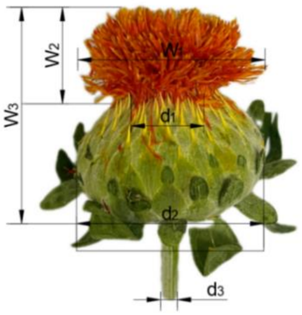

Fig. 1 - The schematic diagram of physical properties of safflower

Table 1

Physical characteristics of safflower

Type	Mean ± standard deviation	95% confidence interval	P value（S-W）
Filament banner(w_1/mm)	32.98 ± 3.7	31.92~34.04	0.38505
Filament length(w_2/mm)	19.12 ± 2.59	18.38~19.86	0.37784
Safflower height(w_3/mm)	40.68 ± 3.38	39.72~41.64	0.14341
Necking Diameter(d_1/mm)	7.54 ± 1.05	7.24~7.84	0.07363
Flower bulb diameter(d_2/mm)	30.58 ± 3.70	29.53~31.63	0.14108
Flower stem diameter(d_3/mm)	3.024 ± 0.41	2.91~3.14	0.77226

Overall structure and principle

As is shown in Figure 2, the safflower harvester is mainly composed of an electronic control system, binocular camera, three-axis robotic arm, rotary cutting safflower harvesting end effector, collection device and walking device.

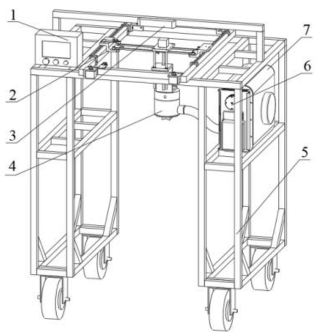

Fig. 2 - The safflower harvester structure schematic diagram

1 - electronic control system; 2 - three-axis robotic arm; 3 - binocular camera; 4 - rotary cutting safflower harvesting end effector; 5 - walking device; 6 - negative pressure fan; 7 - collection device

After the binocular camera acquires the spatial position information of the safflower, the electronic control system adjusts the three-axis robotic arm to align the end effector with the filaments for harvesting, and the cut filaments are collected to the filament collection device through the conveying pipeline under negative pressure fan.

Design and analysis of key components

- ***Rotary cutting end effector structural design***

The structure of the rotary cutting end effector is shown in Figure 3, which mainly consists of stepping motor, transmission gear set, filament feeding status monitoring device, cutting tool, conical feeding device, negative pressure pipeline, cutting disk and housing. Its working principle is: the suction force generated by the negative pressure fan sucks up the safflower filaments and keeps the vertical state. Then the safflower is fed into the feeding device. Meanwhile, the filament feeding status monitoring device real-time monitors the distance between the filaments and the device. When safflower arrives at the appropriate harvesting position, the stepping motor is controlled to start to drive the cutting tool rotating to achieve rotary cutting, so that the filaments and the ball of flower can be separated. Under negative pressure, the separated filaments are adsorbed to the filament collection box through the negative pressure pipeline. The collection of filaments is completed.

The rotary cutting tool is the key component of the filament harvesting mechanism. During operation, the three knives rotate under the motor drive, and the knives hold the filaments to cut them off. Under the adsorption force of the negative pressure fan, the filaments remain vertical and converge, which ensures the integrity of the cut filaments, reduces the damage rate of the filaments and improves the recovery rate. Based on the safflower characteristics, the parameters of the filament harvesting mechanism was designed, and the key factors affecting the recovery rate were determined by analyzing the force and speed of filaments under the action of the rotary cutting tool.

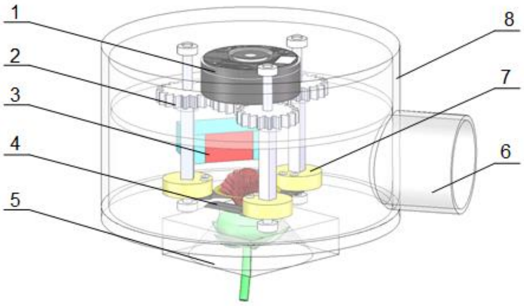

Fig. 3 - The diagram of the rotary cutting end effector

1 - stepping motor; 2 - transmission gear set; 3 - filament feeding status monitoring; 4 - cutting tool; 5 - conical feeding device; 6 - negative pressure pipeline; 7 - cutting disk; 8 - housing

The stepping motor is PM3505 head brushless motor, which is characterized by small size, high torque and light weight. This motor can effectively reduce the volume of the end effector and is more suitable for the field of safflower picking end effector. At the same time, the PM3505 motor is equipped with AS5600 encoder, which can be controlled by the controller to reset the motor after each cutting operation. This function can avoid blocking the flower feeding port, so as to ensure the smooth feeding of filaments for the next cutting. The transmission gear set is connected to the PM3505 head brushless motor, which can adjust the rotation speed of the cutting tool according to the operational requirements. During operation, three knives of the rotary cutting set rotate from the outside to the inside to cut the filament, which can expand the cutting radius of the rotary cutting set. The reset function of the motor and the filament feeding status monitoring device work together to change the saffron filament cutting effect.

- ***Filament clamping cutting analysis***

To avoid the filament sliding out along the blade due to the excessive tilt angle, which can result in uneven resistance to damage the filament *(Pang, 1982)*, the force state of the filament during the cutting process is analyzed to obtain the best cutting effect. As is shown in Figure 4, Take the necking center point *O* as the object of study, the particle *O* is subjected to positive blade pressure F_a, F_b, F_c and blade friction N_a, N_b, N_c of the three knives. Since the initial position angle between each two of the three knives is 120°, both the angle α and the angle β are 30° when all knives are tangent to the necking of the flower bulb (just when the filament begins to be cut). Since the rotation speeds of knife A, knife B and knife C are the same, the positive pressure on the cutting blades of the three are also equal, which means $F_a = F_b = F_c$.

According to the friction equation, the edge friction is shown in Equation (1).

$$N_i = F_i f \tag{1}$$

where: i - the number of knife (*i =a, b, c, corresponding to the knives A, B, C*);

f - friction coefficient of cutting tool on filament.

As the positive pressure F_a, F_b, F_c of the cutting blade are equal, so the blade friction N_a, N_b, N_c of the three are also equal. With the particle *O* as the origin, with the direction of the cutting blade curve and its normal for the *x*, *y* axis respectively to establish a coordinate system, Equation (2), (3) are as follows.

$$N_a \cos\alpha = N_b \cos\beta \tag{2}$$

$$N_a \sin\alpha + N_b \sin\beta = N_c \tag{3}$$

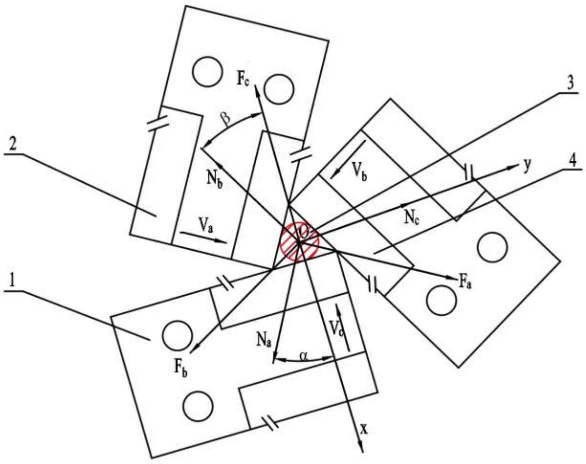

Fig.4 - Force analysis diagram for filament clamping and cutting

1 - knife C; 2 - knife A; 3 - flower bulb necking; 4 - knife B

Combined with the above analysis, the force on the particle *O* is in equilibrium, and the combined force generated by the positive pressure F_a, F_b, F_c and friction N_a, N_b, N_c is in the same straight line. The filaments will remain relatively stable during the cutting process, and will not produce the phenomenon of slippage.

- ***Analysis of cutting resistance of blade***

To reduce the filament damage and fragmentation caused by the impact of the knives, and to reduce the filament damage rate, the composition of the blade cutting resistance force system and the force situation were analyzed. To simplify the analysis model, the cutting force of the three knives is analyzed two by two.

The necking of the flower bulb is a collection of filaments wrapped in sepals, and when cutting filaments from the necking, it is analyzed as a whole unit. When cutting filaments, the cutting blade of the knives and the cutting surface are the main parts that cut off the filaments and withstand the cutting resistance. As is shown in Figure 5, at the moment of cutoff, the cutting resistance of the blade mainly includes: reaction force of the cut filament on the blade R_c, reaction force of the extruded filament on the lower blade R_{zg1}, reaction force of the extruded filament on the lower blade R_{d1}, friction T_1 and pressure of the cutting filament on the upper blade surface *mg,* reaction force of the extruded filament on the upper blade R_{zg2}, reaction force of the extruded filament on the lower blade R_{d2}, friction T_2, just as the Equation (4)~(7) shows.

$$T_1 = fR_1 \tag{4}$$

$$R_1 = R_{zg1} \sin\delta + R_{d1} \cos\delta \tag{5}$$

$$T_2 = f(R_2 + mg\cos\delta) \tag{6}$$

$$R_2 = R_{zg2} \sin\delta + R_{d2} \cos\delta \tag{7}$$

where:

R_1 - reaction force of filaments on the lower blade, [N];

R_2 - reaction force of filaments on the upper blade, [N];

m - quality of filaments, [kg];

f - friction coefficient of blade to filaments.

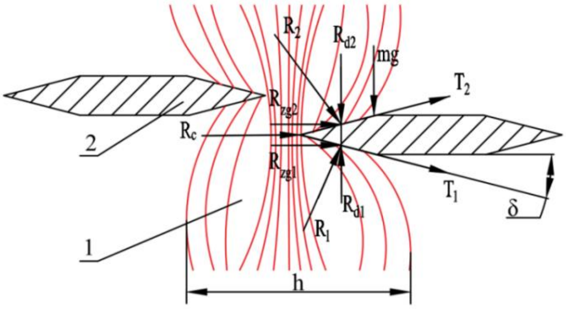

Fig. 5 - Cutting mechanics analysis of blade
1 - safflower filaments; 2 - blade

When extruded, the stress and strain of the filament conforms to the generalized Hooke's law, then the stress-strain relationship when the filaments are extruded by the blade is shown in Equation (8).

$$\varepsilon = \frac{h_{zg}}{h} \approx \frac{\sigma}{E} \tag{8}$$

where: ε- relative density of filaments;

h_{zg} - thickness of extruded filaments on one side of the knife, [mm];

h - total thickness of filaments on one side of the knife, [mm];

σ- extrusion stress on filaments, [Pa];

E - modulus of elasticity of filaments, [Pa].

Substitute equation (8) into equations (5) and (7), according to Pusytgin correlation theory (*Li, B., 2005*), R_{zg1} and R_{zg2}, R_{d1} and R_{d2} are approximately equal respectively. Integrate the unit width dh_{zg} and unit force dR_{zg1}, dR_{zg2} yields Equation (9).

$$R_{zg1} = R_{zg2} = \frac{E}{h}\tan\delta\int_0^{h_{zg}} h_{zg}dh_{zg} = \frac{E}{2h}h_{zg}^{\ 2}\tan\delta \tag{9}$$

The unit reaction force dR_{d1} caused by the lateral pressure of the blade is shown in Equation (10).

$$dR_{d1} = dR_{d2} = \mu\varepsilon E dh_{zg} \tag{10}$$

where: μ - filaments Poisson ratio.

$$R_{d1} = R_{d2} = \mu\frac{E}{h}\int_0^{h_{zg}} h_{zg}dh_{zg} = \mu\frac{E}{2h}h_{zg}^{\ 2} \tag{11}$$

To realize the cutting process, the cutting force P of the blade has to be satisfied with Equation (12)~(13).

$$P \geq R_c + R_{zg1} + R_{zg2} + T_1 + T_2 \tag{12}$$

$$R_c = \Delta l_2 \sigma_s \tag{13}$$

where: Δ- thickness of the blade, [mm];

l_2 - effective length of the blade, [mm].

Cutting resistance is maximized at the point where the neckdown is about to be completely severed, which means $h_{zg} = h$. The cutting force P can be obtained as Equation (14).

$$P = \Delta l_2\sigma_s + EH\left[\tan\delta + f(\sin\delta\tan\delta + \mu c\text{os}\,\delta)\right] + mgf\,\cos\delta \tag{14}$$

According to the physical characteristics of filaments, the modulus of elasticity of filaments is 2.5×10^6Pa, and the Poisson ratio of filaments is 0.25. Substituting the characteristic parameters of filaments into Equation (14), it can be seen that the cutting force P increases with the increase of the inclination angle of the blade, and the trend of the increase is smaller when δ is satisfied with 10°≤ δ ≤20°. Combined with the above analysis, to reduce the cutting force required for separation and to reduce the harvesting damage rate, 10°≤ δ ≤20°was selected as the test factor for filament cutting performance.

- ***Analysis of cutting speed***

To effectively reduce the filament damage rate, the cutting speed of rotary cutting tool was analyzed (*Li et al., 2020*). Since the blade is straight, the radius of rotation at each point of the blade is different when the tool rotates to cut, so the linear velocity *v* is also different. During operation, the safflower was fed by the robotic arm to the appropriate position after the cutting tool rotates and cuts at high speed. The linear velocity v can be calculated by Equation (15).

$$v = 2\pi nr \tag{15}$$

where: n - knife rotational shaft speed, [rpm];

r - actual cutting tool radius, [mm].

Combined with the characteristics of safflower, the actual cutting radius of the tool r ranges from 26 to 40 mm. According to the previous test, knife shaft speed ranges between 1200-1800 rpm. With the Equation (15) for calculating, the blade linear velocity v is 3.27~7.54 $\mathrm{m\ s^{-1}}$. The larger the knife shaft speed *n* is, the larger the blade linear velocity *v* is. Comprehensive analysis of the above, the knife shaft speed *n* was selected as the key factor affecting the effect of harvesting, and the value range is rounded to 1200~1800 rpm.

- ***Design of filament feeding status monitoring device***

The precision of filament cutting position is the key to reduce filament breakage (*Zhang et al., 2022*). The current harvesting method is difficult to meet the demand for accurate positioning, which is easy to cause damage to filament. In this study, a method of infrared sensor to monitor the filament cutting position was proposed. The filament feeding status monitoring device is schematically shown in Figure 6, which consists of detection component, transmitting component and receiving component. According to the real-time monitoring of safflower filaments and infrared sensor distance, it is possible to determine whether the end effector has reached the proper harvesting position (*Zhang et al., 2022*).

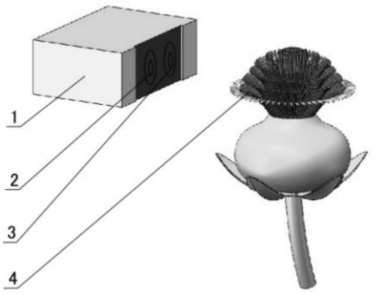

Fig. 6 - Schematic structure of filament feeding status monitoring device

1 - detection component; 2 - transmitting component; 3 - receiving component; 4 - safflower

- ***Simulation analysis of flow field in harvesting chamber***

The flow field generated by the negative pressure collection system is the key to the filament recovery rate. The flow field carries the lightweight filaments through the harvesting chamber and reaches the filament collection box through the conveying pipeline. Fluent software was used to analyze the flow field inside the harvesting chamber to find out the characteristics of the airflow inside the chamber, and the key factors affecting the filament harvesting effect were determined, which provides a theoretical basis for the optimization of the structural parameters of the rotary cutting end effector.

The wind speed is the key parameter that determines whether the filaments can be kept in a vertical state. It also influences whether the cut filaments can be transported to the collection box smoothly. The value is determined by the operating air volume of the negative pressure fan. According to the replacement principle *(Dai, 2008)*, the air volume of the fan should be the volume of the inner chamber of the harvesting device, as is shown in Equation (16).

$$V_f = \frac{Q}{STK} \tag{16}$$

Where: Q - rated air volume of fan, [$\mathrm{m^3}$];

S - inlet cross-section of feeding device, [$\mathrm{m^2}$];

T - the time it takes to cut a safflower down, [s];

K - coefficients that take into account the attenuation of the airflow and losses along the way (K=1.3~1.6).

It was experimentally determined that S = 0.1m^2 and T = 1s. Combined with Equation (16), the wind speed ranges from 3 to 7 $\mathrm{m\,s^{-1}}$.

According to the calculated wind speed, numerical simulation of the chamber flow field under the action of the negative pressure fan was carried out. The velocity distribution vector diagram of the chamber flow field was obtained, as shown in Figure 7. The airflow forms a high-speed area with a large area at the chamber entrance and chamber exit. Due to the existence of the guide port, the flow field layout is relatively straight, which is beneficial to the efficient collection of filaments. The analysis shows that the harvesting end effector chamber and the rotary cutting tool are the key structures affecting the distribution of the flow field for filament harvesting. The fluid motion characteristics inside the chamber is in line with the expected effect, which can realize the function of efficiently collecting safflower.

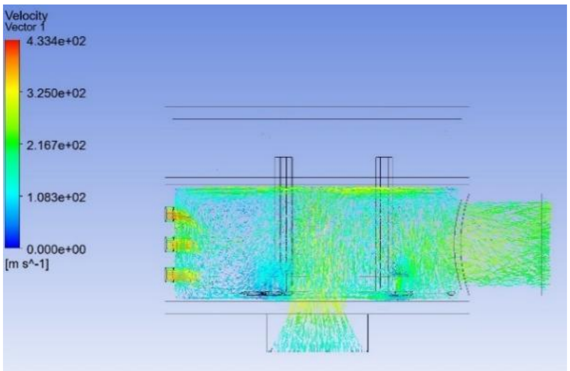

Fig. 7 - Vector diagram of flow field velocity in the harvesting chamber

Experimental materials and equipment

The orthogonal test of cutting end effector was carried out in July 2023 in the laboratory of Northwest Agriculture and Forestry University (NWAFU), and the test safflower was "Yu Hong No. 3" planted by Gongchuang Planting Specialized Cooperative, Yuanzhou District, Guyuan City, Ningxia Hui Autonomous Region. The test equipment is the designed rotary cutting end effector and the collection device, which consists of a centrifugal fan, a lithium battery, a collection box and a collection hose. The test instruments mainly include electronic balance (Suzhou Jutian Instrument and Equipment Co., Ltd., range: 0-3000g, precision 0.01g), SW-6234C tachometer (Speed Group Co., Ltd., range 2.5~99999rpm, precision 0.1rpm) and so on.

Experimental methods

- ***Determination of influencing factors***

Based on the previous analysis, combined with the structure and working parameters of the designed rotary cutting safflower harvesting end effector, the three key factors affecting the harvesting effect were selected as blade inclination, knife shaft speed and wind speed.

(1) Blade inclination: According to the preliminary calculations, the larger the blade inclination, the more unstable the cutting process, which is more likely to push down the filament and cause greater damage to the filament. On the contrary, the smaller the blade inclination, the service life of the cutting tool will be reduced, making the knife easy to break. According to the pre-test, the blade inclination selection range is more suitable within 10°~20°.

(2) Knife shaft speed: The knife shaft speed determines whether the filaments can be cut down smoothly. If the knife shaft speed is too high, the knife will cut the filaments excessively, which will cause some damage to the filaments and make the quality of the harvested filaments poor. If the knife shaft speed is too low, the filaments will be difficult to be cut down smoothly. According to the pre-test, the knife shaft speed is suitable in the range of 1200~1800 rpm.

(3) Wind speed: The higher the wind speed, the more the filaments will be kept in a vertical state into the harvesting chamber, so that the cutting tool will cut down the filaments completely. In this way, the filaments can be collected into the collecting device smoothly, so as to improve the quality of the filaments harvested. If the wind speed is too low, the filaments are more scattered, which will make the cut down filaments more fragmented. The filaments are prone to be retained in the chamber of the end effector, which will result in the loss of filaments, thus making the quality of the collected filaments poorer. According to the pre-test, the wind speed selection range of 3~7$\mathrm{m\,s^{-1}}$ is more appropriate.

- ***Response indicators***

$$y_1 = \frac{m_1}{m} \times 100\% \tag{17}$$

$$y_2 = \frac{m_2}{m_1} \times 100\% \tag{18}$$

$$y_3 = \frac{m_3}{m} \times 100\% \tag{19}$$

where, y_1 - recovery rate, is the percentage of the mass of filaments harvested to the total mass of filaments;

y_2 - damage rate, is the percentage of the mass of filaments that produced damage versus the mass of filaments that were harvested;

y_3 - loss rate, is the percentage of the mass of dropped filaments to the total mass of filaments;

m - the total mass of the filaments, [g];

m_1 - the filaments harvested, [g];

m_2 - the mass of filaments that produced damage, [g];

m_3 - the mass of dropped filaments, [g].

According to the working performance requirements of the rotary cutting safflower harvesting end effector, the test selected the recovery rate y_1, the damage rate y_2 and the loss rate y_3 as the evaluation indexes of the harvesting effect (*Zhang et al., 2022*), which can be obtained by Equation (17)~(19).

- ***Test design***

To analyze the effects of different blade inclination, knife shaft speed and wind speed of rotary cutting safflower harvesting end effector on the performance of safflower harvesting operation, and to find the optimal parameter combination, according to Box-Behnken test theory, three-factor and three-level analysis test was designed, which analyzes the values of test factors. The test factors and levels are shown in Table 2.

Table 2

Test factors and levels

Levels	Blade inclination x_1 (°)	Knife shaft speed x_2 (rpm)	Wind speed x_3 (m s^{-1})
-1	10	1200	3
0	15	1500	5
1	20	1800	7

RESULTS

The test scheme and results are shown in Table 3, with a total of 17 groups of tests, including 12 analytical factors and 5 zero-point estimation errors, with groups 1 to 12 being analytic factorial design tests, and groups 13 to 17 being central design tests (*Wang et al., 2020*).

Test results and analysis

- ***Test program and results***

Table 3

Test results

number	blade inclination x_1	knife shaft speed x_2	wind speed x_3	recovery rate y_1	damage rate y_2	loss rate y_3
1	10	1200	5	90.62	9.11	5.8
2	20	1200	5	87.25	7.32	7.5
3	10	1800	5	91.93	10.21	5.4
4	20	1800	5	91.11	9.62	5.9
5	10	1500	3	90.35	9.44	7.2
6	20	1500	3	89.62	8.53	8.5
7	10	1500	7	92.63	8.72	4.7
8	20	1500	7	90.22	7.65	4.9
9	15	1200	3	86.71	7.72	8.3
10	15	1800	3	88.15	8.64	8.8
11	15	1200	7	86.84	6.46	7.5
12	15	1800	7	91.92	8.52	5.7

number	blade inclination x_1	knife shaft speed x_2	wind speed x_3	recovery rate y_1	damage rate y_2	loss rate y_3
13	15	1500	5	89.01	7.44	6.3
14	15	1500	5	89.24	7.85	6.2
15	15	1500	5	88.86	7.54	5.5
16	15	1500	5	89.07	7.41	5.9
17	15	1500	5	89.42	7.56	5.6

- ***Regression modeling and significance analysis***

The analysis of variance was performed by Design-Expert 8.0 software to establish the coded regression mathematical model of recovery rate, damage rate and loss rate on blade inclination, knife shaft speed and wind speed. Table 4 shows the analysis of variance and significance test of the test results.

As can be seen from Table 4, the fit of the regression model of each factor on recovery rate y_1, damage rate y_2 and loss rate y_3 was highly significant (P < 0.01). For the misfit term, the P value of the three models was greater than 0.05, which was not significant, indicating that the regression model was not misfit. After eliminating the insignificant factors, the regression model of each factor on recovery rate y_1, damage rate y_2 and loss rate y_3 was obtained as Equation (20)~(22).

$$y_1 = 89.12 - 0.92X_1 + 1.46X_2 + 0.85X_3 + 0.64X_1X_2 - 0.42X_1X_3 + 0.91X_2X_3 + 1.70X_1^2 - 0.60X_2^2 - 0.12X_3^2 \tag{20}$$

$$y_2 = 7.56 - 0.54X_1 + 0.80X_2 - 0.37X_3 + 0.30X_1X_2 - 0.040X_1X_3 + 0.28X_2X_3 + 1.13X_1^2 + 0.38X_2^2 - 0.10X_3^2 \tag{21}$$

$$y_3 = 5.90 + 0.46X_1 - 0.41X_2 - 1.25X_3 - 0.30X_1X_2 - 0.28X_1X_3 - 0.57X_2X_3 - 0.50X_1^2 + 0.75X_2^2 + 0.93X_3^2 \tag{22}$$

From the analysis of F value of each factor in Table 4, it can be seen that the three factors affecting the recovery rate are knife shaft speed, blade inclination, and wind speed in descending order of importance. The damage rate is affected by knife shaft speed, blade inclination, and wind speed in descending order of importance. And the loss rate is affected by wind speed, knife shaft speed, and blade inclination in descending order of importance.

Table 4

Analysis of variance of the test results

origin	recovery rate		damage rate		loss rate	
	F value	P value	F value	P value	F value	P value
model	55.30	<0.0001	70.78	<0.0001	15.56	0.0008
X_1	68.91	<0.0001	98.13	<0.0001	8.46	0.0168
X_2	175.26	<0.0001	210.13	<0.0001	8.86	0.0271
X_3	58.95	0.0001	45.84	0.0003	71.28	<0.0001
$X_1.X_2$	16.68	0.0047	14.87	0.0062	2.05	0.1950
$X_1.X_3$	7.24	0.0311	0.26	0.6230	1.73	0.2305
$X_2.X_3$	33.98	0.0006	13.42	0.0080	7.54	0.0287
X_1^2	125.40	<0.0001	221.05	<0.0001	6.00	0.0441
X_2^2	15.36	0.0058	24.78	0.0016	13.51	0.0079
X_3^2	0.61	0.4607	1.83	0.2185	20.54	0.0027
lost proposal	3.54	0.1267	0.53	0.6864	1.94	0.2650

highly significant (P <0.01); insignificant (P≥0.05); X_i is the level value of x_i, i=1,2,3.

- ***Effect of interaction factors on response functions***

The effects of the three-factor interaction on the recovery rate are shown in Figure 8(a)~(c). From Figure 8(a), it can be seen that when the wind speed is fixed at 0 level (x_3 = 5 $\mathrm{m\ s^{-1}}$), the response surface curve changes faster along the direction of the blade inclination, which means the effect of the blade inclination on the recovery rate is more significant. From Figure 8(b), it can be seen that when the knife shaft speed is fixed at 0 level (x_2 = 1500 rpm), the response surface curve changes faster along the direction of the blade inclination, which means the effect of the blade inclination on the recovery rate is more significant.

From Figure 8(c), it can be seen that when the blade inclination is fixed at 0 level (x_1 = 15°), the response surface curve changes faster along the direction of the knife shaft speed, which means the effect of the knife shaft speed on the recovery rate is more significant. Therefore, under the premise of meeting the requirements of the recovery rate, a higher knife shaft speed is selected.

The effects of the three-factor interaction on the damage rate are shown in Figure 8(d)~(f). From Figure 8(d), it can be seen that when the wind speed is fixed at 0 level (x_3 = 5 $\mathrm{m}\ s^{-1}$), the response surface curve changes faster along the direction of the blade inclination, which means the effect of the blade inclination on the damage rate is more significant.

From Figure 8(e), it can be seen that when the knife shaft speed is fixed at 0 level (x_2 = 1500 rpm), the response surface curve changes faster along the direction of the blade inclination, which means the effect of the blade inclination on the damage rate is more significant. From Figure 8(f), it can be seen that when the blade inclination is fixed at 0 level (x_1 = 15°), the response surface curve changes faster along the direction of the knife shaft speed, which means the effect of the knife shaft speed on the damage rate is more significant. Therefore, under the premise of meeting the requirements of the damage rate, a smaller blade inclination is selected.

The effects of the three-factor interaction on the loss rate are shown in Figure 8(g)~(i). From Figure 8(g), it can be seen that when the wind speed is fixed at 0 level (x_3 = 5 $\mathrm{m}\ s^{-1}$), the response surface curve changes faster along the direction of the knife shaft speed, which means the effect of the knife shaft speed on the loss rate is more significant. From Figure 8(h), it can be seen that when the knife shaft speed is fixed at 0 level (x_2 = 1500 rpm), the response surface curve changes faster along the direction of the wind speed, which means the effect of the wind speed on the loss rate is more significant. From Figure 8(i), it can be seen that when the blade inclination is fixed at 0 level (x_1 = 15°), the response surface curve changes faster along the direction of the wind speed, which means the effect of the wind speed on the loss rate is more significant. Therefore, under the premise of meeting the requirements of the loss rate, a higher wind speed is selected.

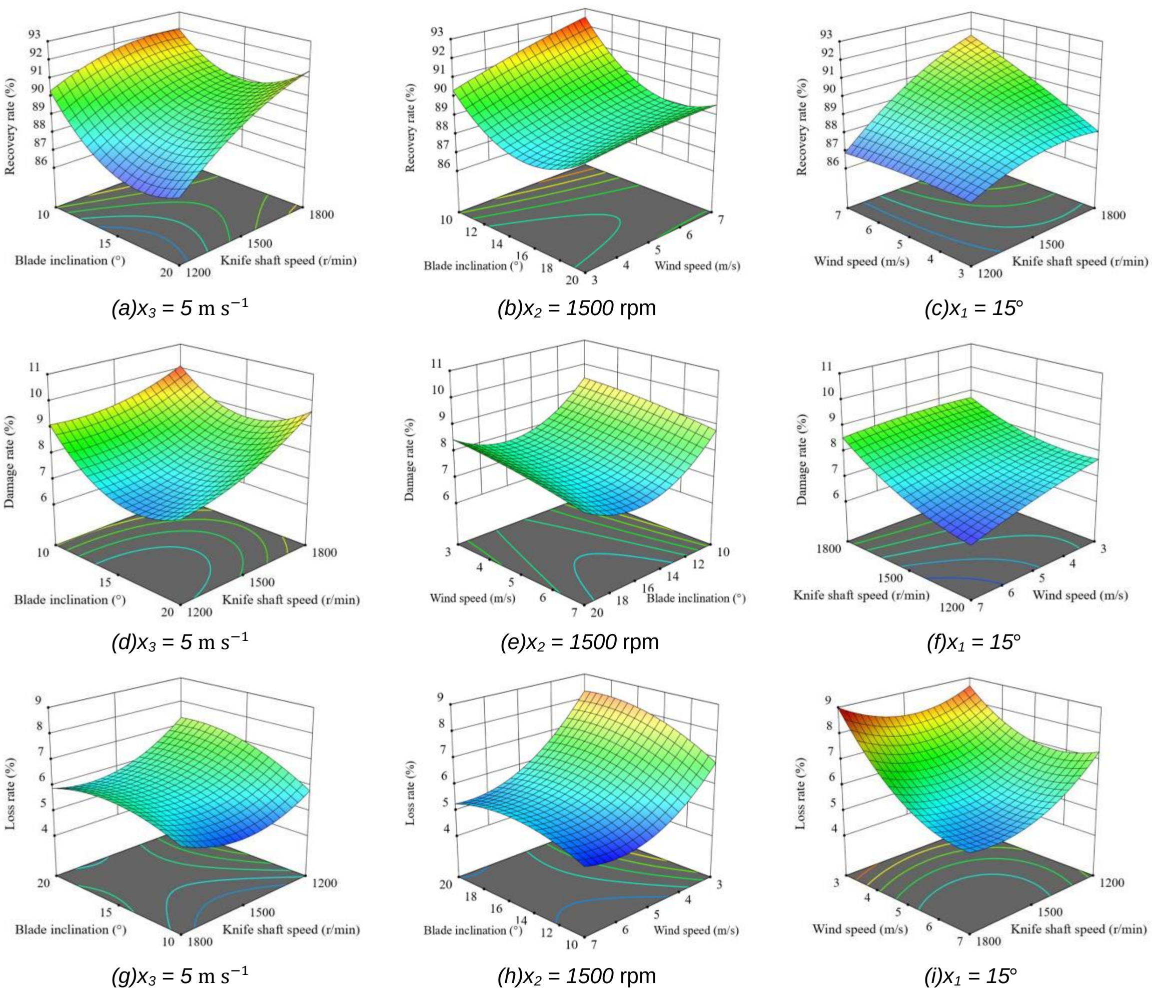

(a)x_3 = 5 $\mathrm{m\ s^{-1}}$ *(b)x_2 = 1500* rpm *(c)x_1 = 15°*

(d)x_3 = 5 $\mathrm{m\ s^{-1}}$ *(e)x_2 = 1500* rpm *(f)x_1 = 15°*

(g)x_3 = 5 $\mathrm{m\ s^{-1}}$ *(h)x_2 = 1500* rpm *(i)x_1 = 15°*

Fig. 8 - Effect of interaction factors on response functions

Parameter optimization and validation

- ***Parameter optimization***

To ensure that the rotary cutting safflower harvesting end effector has better working performance, according to the objectives of high recovery rate, low damage rate and low loss rate, the structure and working parameters of the end effector were optimized.

The optimization solution was carried out by using the Optimization-Numerical module in Design-Expert 8.0. The objective function and constraints are shown in Equation (23).

$$\begin{cases} \max y_1(x_1, x_2, x_3) \\ \min y_2(x_1, x_2, x_3) \\ \min y_3(x_1, x_2, x_3) \\ 15 \le x_1 \le 20 \\ 1200 \le x_2 \le 1800 \\ 3 \le x_3 \le 7 \end{cases} \tag{23}$$

After optimization, the best parameter combinations of influencing factors were obtained as follows: blade inclination is 15.31°, knife shaft speed is 1566.63 rpm, wind speed is 6.13 $\mathrm{m}\ s^{-1}$. At this time, the model predicted that the recovery rate was 92.88%, the damage rate was 7.79%, and the loss rate was 4.88%.

- ***Verification test***

The test validation was carried out in July 2023 in Gongchuang Planting Specialized Cooperative, Yuanzhou District, Guyuan City, Ningxia Hui Autonomous Region, rounding the optimized parameter combinations to blade inclination of 15°, knife shaft speed of 1570 rpm, and wind speed of 6 $\mathrm{m\ s}^{-1}$. The test site is shown in Figure 9.

Fig.9 - Field trial validation

To eliminate random errors, the test was repeated 10 times under this parameter combination. And the results were averaged. The recovery rate was 91.47%, the damage rate was 7.51%, and the loss rate was 4.67%. The relative errors with the theoretical optimized values were 0.6%, 0.9%, and 1.5%, respectively, which indicated that the resulting optimal parameter combinations could satisfy the requirements of practical applications.

CONCLUSIONS

(1) Aiming at the problems of high damage rate and low recovery rate during safflower harvesting, this study designed a rotary cutting safflower harvesting end effector. After the filament feeding status monitoring device monitors that the filament arrives at the suitable cutting position, the motor drives the three knives to rotate to realize the cutting of the filament, which can effectively reduce the filament damage rate and improve the recovery rate.

(2) By establishing the mechanical model of tool-filament cutting, the dynamics of filament cutting process was analyzed. According to the theoretical analysis and calculation, it was determined that the blade inclination and the knife shaft speed were the key factors affecting the harvesting effect. Simulation was carried out to analyze the characteristics of the flow field inside the harvesting chamber, and the inlet wind speed was determined as the key factor affecting the harvesting effect.

(3) The Design-Expert software was used to analyze the effects of blade inclination, knife shaft speed and wind speed of the harvesting device on the recovery rate, damage rate and loss rate, respectively. A cubic regression model was constructed to optimize the structure and working parameters of the harvesting device, so as to obtain the optimal parameter combinations of blade inclination of 15 °, knife shaft speed of 1570 rpm and wind speed of 6 $\mathrm{m\,s^{-1}}$. The validation test was carried out in the field. The recovery rate, damage rate and loss rate are 91.47%, 7.51% and 4.67%, respectively, which can meet the requirements of parameter optimization of rotary cutting safflower harvesting end effector.

(4)

ACKNOWLEDGEMENT

The authors appreciate the financial support provided by the National Natural Science Foundation of China (32272001) and the Qinchuangyuan Project of Shaanxi Province (2023KXJ-016).

REFERENCES

[1] Cao, W., Yang, S., Li, S., Jiao, H., Lian, G., Niu, C., An, L. (2019). Parameter optimization of height limiting device for comb-type safflower harvesting machine (梳夹式红花采收机等高限位装置参数优化). *Transactions of the Chinese Society of Agricultural Engineering*, Vol.35, Issue 14:48-56;

[2] Dai, F. (2008). Selection and calculation of the blowing rate of air-assisted sprayers (风送喷雾机风量的选择与计算). *Plant Protection*, Issue 06:124-127;

[3] Hu, G., Bu, L., Chen, J. (2020). Simulation to determination of significant parameters on apple stress for combing harvesting in trellis trained trees. *Scientia Horticulturae*, Vol.274;

[4] Hu, G., Chen, C., Chen, J., Sun, L., Sugirbay, A., Chen, Y., Jin, H., Zhang, S., Bu, L. (2022). Simplified 4-DOF manipulator for rapid robotic apple harvesting. *Computers and Electronics in Agriculture*, Vol.199;

[5] Hu, G., Zhang, E., Zhou, J., Zhao, J., Gao, Z., Sugirbay, A., Jin, H., Zhang, S., Chen, J. (2021). Infield Apple Detection and Grading Based on Multi-Feature Fusion. *Horticulturae*, Vol.7, Issue 9;

[6] Jobbagy, J., Martin, D., Koloman, K., Patrik, B. (2021). Mechanized Grape Harvest Efficiency. *Applied Sciences-Basel*, Vol.11, Issue 10;

[7] Joao, P., Martins, D., Cunha, W. (2011). Operational performance of the mechanized and semi-mechanized potato harvest. *Engenharia Agricola,* Vol.31, Issue 4:826-834;

[8] Li, B. (2005). *Research on the One-Sheet Hyperboloid Cylindrical Cutter with Flat Surface and Straight Edge (单叶双曲面平板直刃滚筒式切碎器的研究)*. PhD dissertation, China Agricultural University, Beijing/China;

[9] Li, S. (2005). Safflower 2005' became popular (红花2005'走红). *Modern Chinese Medicine*, Issue 06:50;

[10] Li, T., Meng, Z., Ding, H., Hou, J., Shi G., Zhou K. (2020). Mechanical analysis and parameter optimization of cabbage root cutting operation (甘蓝切根作业力学分析与参数优化). *Transactions of the Chinese Society of Agricultural Engineering*, Vol.36, Issue 07:63-72;

[11] Pang, S. (1982). Slip Shear Theory and Selection of Slip Shear Angle (关于滑切理论与滑切角的选用). *Journal of Huazhong Agricultural College*, Issue 02:64-69;

[12] Pu, Y., Wang, S., Yang, F., Ehsani, R., Zhao, L., Li, C., Xie, S., Yang, M. (2023). Recent progress and future prospects for mechanized harvesting of fruit crops with shaking systems. *International Journal of Agricultural and Biological Engineering*, Vol.16, Issue 1;

[13] Ren, C., Wu, Y., Tang, X., Hu, J., Chen, J., Wu, Q., Pei, J. (2017). Safflower's origin and changes of producing areas (红花的起源与产地变迁). *China Journal of Chinese Materia Medica*, Vol.42, Issue 11:2219-2222;

[14] Wang, F., Wang, D. (2020). Design and test of 4TSQ-2 sugar beet top cutter (4TSQ-2型甜菜切顶机设计及试验). *Transactions of the Chinese Society of Agricultural Engineering*, Vol.36, Issue 02:70-78;

[15] Wang, J., Pang, X., Hu, Y. (2006). An analysis on ecological and climatic conditions for cultivation Carthamus tinctorius L in alar irrigated area (阿拉尔垦区红花栽培气候生态条件分析). *Agricultural Research in the Arid Areas*, Issue 03:42-44+53;

[16] Xue, X., Zhang, M. (2005). The main nutrients and utilization value of Xinjiang safflower (新疆红花的主要营养成分及利用价值). *Food and Nutrition in China*, Issue 12:40-42;

[17] Zhang, S., Chen, Q., Liu J., Chen, Y., Chen, J., Jin, H., Luo, T. (2021). Research on design and experiment of multifunctional vegetable filed machine. *INMATEH-Agricultural Engineering*, Vol.63 (1), 434-442;

[18] Zhang, T., Zhang, L., Ge, Y., Liu, G., Zhang, X. (2020). Development and Test of a Portable Roller-type Safflower Harvester (便携对辊式红花采收机的研制与试验). *Journal of Agricultural Mechanization Research*, Vol.42, Issue 03:76-81;

[19] Zhang, X., Ge, Y., Chen, F., Yu, P. (2022). Design of Three-Finger Pull-Out Safflower Picking End Effector (三手指拉拔式红花采摘末端执行器的设计). *Machinery Design & Manufacture*, Issue 01:145-149;

[20] Zhang, X., Zhang, H., Shi Z., Jin, W., Chen, Y., Yu, Y. (2022). Design and experiments of seed pickup status monitoring system for cotton precision dibblers (棉花精量穴播器取种状态监测系统设计与试验). *Transactions of the Chinese Society of Agricultural Engineering*, Vol.38, Issue 05:9-19;

[21] Zhang Z., Lv, Q., Ren, J., Han, C., Yuan, P., Zhang, X. (2019). Design of critical components for safflower harvesting machinery by rotary shear (旋转剪切式红花花丝采摘机械关键部件的设计). *Journal of Chinese Agricultural Mechanization*, Vol.40, Issue 07:1-6;

[22] Zhang, Z., Zhao, M., Xing, Z., Liu, X. (2022). Design and Test of Double-acting Opposite Direction Cutting End Effector for Safflower Harvester (红花采收机双动对切式末端执行器设计与试验). *Transactions of the Chinese Society for Agricultural Machinery*, Vol.53, Issue 12:160-170;

[23] Zhou, Y., Guo, J., Ma, X., Fan, X., Chen, Y., Lin, M. (2021). Research on Current Situation and Development Countermeasures of Xinjiang Safflower Production (新疆红花生产现状及发展对策研究). *Journal of Anhui Agricultural Sciences*, Vol.49, Issue 19:199-201+217.